STATEMENT

Name: Ivan Contini Abilio
Neptun ID: NHIBNX

ELTE Faculty of Science, specialization: MSc in Material Sciences

Title of diploma work: Numerical Simulation of Topological Materials

As the author of the diploma work, I declare, with disciplinary responsibility that my thesis is my own intellectual product and the result of my own work. Furthermore, I declare that I have consistently applied the standard rules of references and citations.

I acknowledge that the following cases are considered plagiarism:
– using a literal quotation without quotation mark and adding citation;
– referencing content without citing the source;
– representing another person's published thoughts as my own thoughts.

Furthermore, I declare that the printed and electronical versions of the submitted diploma work are textually and contextually identical.

Budapest, December 29, 2020

Signature of Student

EOTVÖS LORÁND UNIVERSITY

MSc in Material Sciences

THESIS

Numerical Simulation of Topological Materials

Author:
Ivan Contini Abilio

Internal Supervisor:
Katalin Sinkó
External Supervisor:
Gábor Széchenyi

2021

"It is clear today that modern science developed when people stopped debating metaphysical questions about the world and instead concerned themselves with the discovery of laws that were primarily mathematical."

Mordechai Ben-Ari

TABLE OF CONTENTS

ABSTRACT

To observe and study the behavior of Majorana wires, we use numerical simulations with the system using a Kitaev Chain model through the second quantization formalism as one of the possible bases for quantum computing. Due to the degeneracy of the ground state in the Majorana Wire, a direct measurement of its parity is not possible, so both ends of the wire are connected to a quantum dot. These connections are controlled so they are only open in "Pulses" magnetically controlled, of which the Strength and Duration are controllable, the former forming the Hopping Parameter for the system, and they affect when the quantum dot is filled. Each different parity will have different probabilities of filling the quantum dot depending on the values of such parameters, each accompanied by a Parity Readout Error chance. The quantum dot itself presents a random factor due to its varying possible On-site energy. To find the best parameters taken into account the random nature of the probabilities found, we simulated multiple iterations, with 5000 realizations each. As the main result, we can optimize the results of the Parity Readout Error concerning the length and strength of the tunneling pulses. We generalized previous studies by taking into account non-symmetric tunneling pulses and on-site detuning.

Keywords: Numerical Simulation; Majorana; Majorana Wire; Topological Materials;

1. Introduction

Since its invention during the 1960s, modern computers have advanced greatly in both power and efficiency. While there were other forms of computational technologies before, it was only in the 1960s that the modern computer system took form thanks to the invention of Walter Brattain and John Bardeen: the transistor. Before the invention of transistors engineers and scientists had to use vacuum tubes, which are much bigger and slower than transistors, which greatly diminish the potential for computers. Now with the transistors, which could be easily mass-produced, and would prove to be able to be greatly miniaturized, the computational revolution could start. Nowadays computer devices with greater processing capacities than the ones that occupied entire rooms can be found in almost anybody's pocket, and electronic devices are now essential to the workings of the modern world. However, as they become more and more common and necessary, it has been requested of them more and more processing power in smaller sizes.

This has led to greater and greater miniaturization of the processing units, and therefore of the transistors, to increase their processing capacity per area, but this miniaturization has its problems. Beyond the problem of overheating that these systems become to have increased propensity as more transistors are placed together, this miniaturization is reaching a limit in size. Nowadays still experimental transistors are reaching sizes of about 5-7 nm[1], but this is seen to be the limit size for traditional transistors, as around 5nm quantum tunneling starts to happen and affect the uses of the transistor[2]. Many before had claimed that around 2021 continuous research for the miniaturization of traditional transistors would become “economically undesirable” due to reducing returns[3]. This has led many to look for different alternatives for the

traditional transistors[4], and along with them, there is the possibility of the use of quantum computing.

Quantum computing is a relatively new technology that develops techniques and technologies that can use quantum effects on the improvement and construction of computers. Credited to have started in 1980 by Paul Benioff's proposal to use a quantum mechanical model for the Turing Machine[5], since then it has developed greatly and many different lines of research exist. As all these lines develop and improve, quantum technologies have shown to be theoretically not only capable to have as much processing power as traditional computing, but have recently shown in practice to be so. The Sycamore processor produced by Google[6] and a Chinese Photonic quantum computer[7] have both claimed "Quantum Supremacy" in 2020, which means that their quantum computers can now perform processes that "no classical computer can perform the same task in a reasonable amount of time and is unlikely overturned by classical algorithmic or hardware improvements"[7].

Besides that, quantum technologies are still very much experimental, as they are affected by many difficulties that traditional systems don't, especially on control and maintenance of the systems. Due to the nature of the quantum system, they need to deal with nanometric systems, and beyond the natural difficulty of working at such a small scale, systems at this size are very sensitive to any external noise or background effect. This all makes that these technologies need to be worked on isolated conditions, shielded against electromagnetic fields and environmental noise, and cooled to near absolute zero. This all makes these systems very complex and costly to build and if quantum computing is to become a possible replace, or even supersede, traditional technologies it has to become more resilient to perturbances.

All electronic devices use binary bits as the bases for all their processes, and in traditional computing they are represented by electricity (or lack thereof) through semiconducting lines or the polarity of a material in a metallic plate. Some quantum computer technologies use qubits instead, using some form of quantum particle or state to represent the same binary information in one of many ways. These qubits are often one of the most sensitive parts of the system, as they need to be able to not only be reliably read and reliably stored (even if temporarily) but also able to be easily and quickly rewritten. With that in mind, many researchers are focused on finding a way to make these qubits more resilient to perturbance. This work explores the possible solution of the use of Majorana wires, a specific kind of quantum device which uses the unique properties of Majorana particles and could allow the production of more efficient and functional quantum computers.

1.1. Majorana Anyons

Anyons are a kind of quasiparticle, neither a fermion nor a boson, that cannot exist in the 3D world, only in the 2D, and whenever two Anyons swap positions they change their wave functions[8]. This allows them to be used to do what is called *Braiding*, changing the sequence of a series of Anyons by swapping their positions, creating a unique combination and structure. This cannot be done by either fermions or bosons, as exchanging the position of 2 particles twice in 3D ends with no difference from the original condition[9]. This, however, requires that the system remains in 2D, which can be done by the use of Topological Materials.

Topological materials are materials which properties do not change with their topology, and the most common example is the topological insulators, which are insulators in the bulk but conductive on the surfaces[10, 11]. Topological materials are

called that because their special properties are linked to their topology, and as long as their topology is maintained (that is, in any shape as long as their surface is not broken) they maintain their properties. One of these topological properties, that arrives when a chain of certain materials is placed in proximity of a s-wave superconductor, is the ability to create vortices, a natural quantum defect of superconductors, that can bind Anyons, an exotic kind of theorized particle that can be used for computing[9].

Computers that would use this technology are called topological quantum computers, and they can use these captured particles as qubits, the fundamental part of a quantum computer, analogous to bits to regular computers. These particles can be "moved" around each other, changing their specific states, so they can be "braided", forming into different combinations that can be used to store and calculate information[9]. For these braids to be possible to occur it is necessary some very specific conditions, which include the necessity of anyons, an elusive kind of particle of which few kinds have been theorized.

Majorana Anyons, also known as Majorana particles, is an example of theorized anyon that would have the unique property of being their own antiparticle, in direct opposition to Dirac fermions. Majorana anyons have been theorized first by Ettore Majorana in 1937 in his paper "A symmetric theory of electrons and positrons"[12] as he finds a solution to the Dirac equation were fermions are their own antiparticles, coming to the point to present in its summary "[…] there is no longer any reason to speak of negative-energy states nor to assume, for any other types of particles, especially neutral ones, the existence of antiparticles […]"[12]. Often Majorana particles will be called "Majorana Fermions", although this is an erroneous naming, as two Majorana particles are created by changing the statistics from fermionic to non-abelian statistics.

Nowadays it is known that all fermions on the Standard Model are Dirac fermions, with exception of neutrinos which still require more research to be defined as one or another, and Majorana particles have yet to be confirmed. It has been theorized, however, that under certain conditions, a fermion can separate into two parts, known as Majorana Zero Modes (MZM), when in a superconductor, and many have researched into such possibility, with promising results[12]. Although MZMs will always appear as bounded pairs, multiple pairs in a chain can be manipulated to reform these pairs with MZMs in different sites[13], leaving an unbounded single MZM at the end of the chains, as in **Figure 1.** This process can be well seen in the steps to transition the fermionic statistics to non-abelian statistic, done by the following steps [14]:

- Starting with the Dirac fermionic operators, $\hat{a}\ \hat{a}^{+}$, which represent annihilation and creation of a fermionic particle, respectively. $(\{\hat{a}^{+},\hat{a}^{+}\}=\{\hat{a},\hat{a}\}=0,\{\hat{a},\hat{a}^{+}\}=1)$.

- From there we get the Majorana operators $\frac{\gamma_1}{\sqrt{2}}=\hat{a}+\hat{a}^{+}=\frac{{\gamma_1}^{+}}{\sqrt{2}}$, $\frac{\gamma_2}{\sqrt{2}}=\frac{(\hat{a}-\hat{a}^{+})}{i}=\frac{{\gamma_2}^{+}}{\sqrt{2}}$. As can be seen, the creation and annihilation operators for the Majorana are the same.

- It also gives that $\{\gamma_k,\gamma_l\}=2\delta_{k,l}$, ${\gamma_1}^2={\gamma_2}^2=1$, $\gamma_1\gamma_2=-\gamma_2\gamma_1$, $\hat{a}=\frac{\gamma_1+i\gamma_2}{2}$, $\hat{a}^{+}=\frac{\gamma_1-i\gamma_2}{2}$. This means that with one fermionic operator, there are two Majorana particles, or MZM's.

The resulting Majorana Anyons are localized, but still can be moved far away from each other[14], as well as being greatly resistant to the two most common forms of error in the quantum states used as qubits: the classical error, when there is a flip on the

qubit changing its value from one to 1 to 0 or vice versa; and the phase error, when there is a flip on all the qubits equal to 1 relative to those equal to 0[15].

This great resilience has not passed unnoticed by the researchers, many of who are looking at how to apply it for the construction of devices for quantum computers that are more resilient to decoherence, especially for quantum memory[6, 13]. One of the possible technologies that can use this is Majorana Wire, a cutting-edge topic of research that can reliably create and store MZMs.

1.2. Majorana Wires

A Majorana Wire is a device composed of a 1D nano-sized semiconductor wire in a superconductive substrate with a controllable external magnetic field that can be applied to it. This specific construction allows the semiconducting wire to behave as a Topological Material, sharing properties of both its semiconducting nature and the superconducting substrate where it lays. With the controlled application of a magnetic field over this system, the wire becomes a topological superconductor and has the conditions necessary for the creation of the unpaired MZMs at the ends of the wire that can be "stored" at the end of the chain formed by the 1D semiconductor wire and then "re-pair" them [16]. This leaves non-locally bounded MZMs at the edges of the wire that can be used to store information as qubits that can be safely stored and easily measured. To do so, different designs for the Majorana wire have been conjectured in different

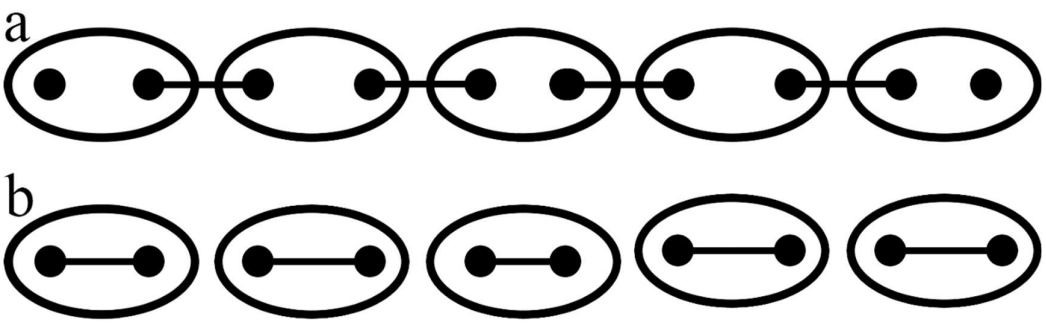

Figure 1: Representation of a Kitaev Chain for the Majorana Wire in two different forms of pairing, one with inter-site cooper pairings, the other with intra-site. Ellipses are sites, solid circles are MZM, straight lines are couplings. Pairing a has one unbounded MZM's at the end of each chain.

experiments to try to observe and detect the MZM's[16, 17], through different methods, including and although some have shown some promise in being able to detect an MZM[18] it has not been proven yet.

The construction of such devices, however, is a difficult affair, from both a standpoint of complexity and cost, but it is possible to numerically simulate the behavior of such devices and gather some important understanding and information about it. These simulations allow us to predict and evaluate the behavior of the fermions at the edges of the Majorana Wire in different conditions and regimes with minimal cost. To do so it is necessary to a formalism and a model, both that ideally fit well with the presented physical system and that can be easily understood. The system is chosen, which is the typical system utilized for this kind of system, is the Kitaev Chain Model through the Second Quantization formalism.

1.3. Second Quantization & the Kitaev Chain

Kitaev Chain is a model created by Alexei Kitaev in 2001 in the paper "Unpaired Majorana anyons in quantum wires"[15]. As the name says, the work is direct to the work with quantum wires, and the model there presented was specifically created to represent Majorana wires and work is within it. The system is composed of a series of 0D sites organized side by side in a 1D line, forming a "chain", and each site can fit two MZM. These MZMs are always bounded to one another, either in the same site or in a different site, forming two kinds of pairing (**Figure 1**). The second kind leaves one unbounded MZM at each end of the chain, which will be used for the qubit to the system.

The system can exist in two different phases with different parities: even and odd (**Figure 1**, **a** and **b** respectively), with these parities forming the bases for the qubits

of the system. These parities, however, are not related to the number of MZM's in the system, as the creation of MZM's always creates two of them from one fermionic operator. This parity is related to the number of fermionic operators in the system, which will depend on the specific coupling between the MZM's. The first phase, presented in **Figure 1 (a)** represents the system with all the MZM's paired in-site, and it is the even parity system. The second phase, presented in **Figure 2**, shows MZM's coupled between sites, leaving two MZM's uncoupled at the ends of the wires, and it represents the odd parity of the system[14]. These two states will work as the "0" and "1" states of the qubit system, just as in traditional computers electric current and lack thereof work as their "1" and "0" states. There is also a special advantage, as superposition allows multiples states to "stack" onto one another, allowing multiple results to be compiled on the same qubit, expanding considerably the capacity of the system.

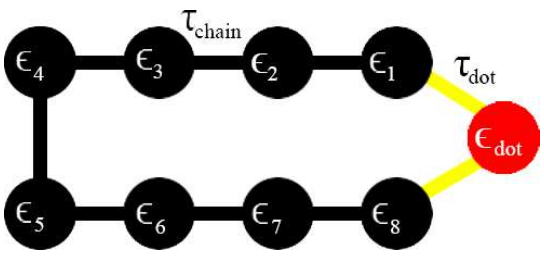

Figure 2: Representation of the Kitaev Chain with 8 sites and an added quantum dot to both its ends. If the Kitaev chain is on the Ideal Kitaev Limit ϵ_1 to ϵ_8 are 0, and all tunneling between sites within the chain are equal to $\tau_{chain} = 1$.

When using the Kitaev Chain model the representations are done by the Second Quantization formalism, which allows representing the state of each site as well as easily represent the possible operations applied to the sites. This model of representation can be used to represent both bosons and fermions, but given that this work focuses on Majorana anyons, the uses with bosons will not be discussed. A system of size *n* is represented by a series of *n* numbers representing the state of each site within a *ket*. Each site on a system can be considered to be either occupied or not occupied by

one fermion, represented by a 1 or 0 to on the position of the site. As an example, in a 3 sites system, with 1 fermion in the first and second site would be represented by:

$$|1,1,0\rangle$$

Representation 1: System with 3 sites with two fermions, at the first and second sites.

All sites can be represented in such a manner, but the *vacuum state*, which is a state where there is no filled site, is usually represented as $|vac\rangle$ independently of the size of the system. Operators can be applied to these states to represent the filling and emptying of sites, respectively a creator and an annihilation operator. These operators are represented by a $c_j^\dagger$ and a c_j, respectively, where the j represents the site position (counted from right to left). Creation operators can only affect empty sites and annihilation operators can only affect filled sites. Any attempt to apply an operator to an invalid site is considered invalid and results in an invalid operation, represented by a single 0.

$$c_1^\dagger|0,1,0\rangle \rightarrow |1,1,0\rangle$$

Representation 2: 3 sites system with one fermion at position two being operated by a creation operator at position 1, leading to a system with sites 1 and 2 filled.

$$c_1^\dagger|1,1,0\rangle \rightarrow 0$$

Representation 3: 3 sites system with two fermion at position one and two being operated by a creation operator at position 1, leading to a invalid operation.

Multiple operators can be represented affecting the same system, with the operations being considered to happen in sequential order. Any system of n size can be represented by any other system of the same size with a sequence of operators. Operators can, however, make the system end in an antisymmetric state depending on the order that the operations happen, in which case there will be a "-" signal representing the "-" for the wavefunction amplitude.

$$|1,1,1\rangle = c_3^\dagger c_1^\dagger|0,1,0\rangle$$

Representation 4: 3 sites system with all sites filled by fermions is equal to 3 sites system filled at position 2 being affected by two creation operators at position 1 and 3.

$$c_1^\dagger c_3^\dagger|0,1,0\rangle \rightarrow -|0,1,0\rangle$$

Representation 5: 3 sites system with a fermion at position two being operated by creation operators at position 3 and 1, leading to an antisymmetric 3 site system with a fermion at position 1.

A system will have a number of different states equal to 2^n, where *n* represents the number of sites available on the system. For an example of the basis states of a 2 sites system there are only the following 4 states possible:

|0,0> |1,0> |0,1> |1,1>

Representation 6: All possible basis states for a 2 sites system (from right to left): vacuum state, one fermion at first position, one fermion at second position, fully filled.

Given that any system can be turned into another by the proper application of creation and annihilation operators, there are many that a state can become another one, so the workings of these operators can be represented by a matrix operator. This is a square matrix with 2^n rows, which lines and columns represent, respectively, the original state in which the operator is being applied and the resulting state of the operation. Cells that represent that this operator can be applied to the original state to transform it into a different state are filled with a 1, and otherwise left empty with a 0, and often only a single cell in each row will be filled. Fully empty rows represent that this operation on this original state is invalid.

This matrix operator is represented with a column representing all the possible base states of the affected system just at the left of the matrix. A matrix operator for the $c_1^\dagger$, that is, the creation operator for the first site, applied to a 2 sites system, can be represented by:

$$\begin{pmatrix} 0 & 1 & 0 & 0 \\ 0 & 0 & 0 & 0 \\ 0 & 0 & 0 & 1 \\ 0 & 0 & 0 & 0 \end{pmatrix} \begin{matrix} |0,0> \\ |1,0> \\ |0,1> \\ |1,1> \end{matrix} \rightarrow \begin{matrix} |1,0> \\ 0 \\ |1,1> \\ 0 \end{matrix}$$

Representation 7: Matrix operator for a creation operator operating in a two site system.

The same for a matrix can be applied to any operator to any system of any size, but as systems become linearly larger the matrixes become exponentially larger. A single matrix can represent a sequence of operators being applied to a single system,

and this matrix can be calculated by applying a matrix dot operation on the individual matrixes in the sequence they are applied to the system. If a sequence of operations would lead to a negative value for the amplitude of the wave function, the filled cell in the matrix will be represented by a -1.

This formalism allows us to represent very well a system within the Kitaev Chain model, Majorana wire included, and using this formalism we can also represent the energetic state of the system. To do so it is necessary to add energy parameters to the system, representing the different energy values of different parts of the system, to different components of the model that represent each different part of the system. The following Hamiltonian is for a Kitaev Chain of N sites, formed using the Second Quantization formalism[17, 19, 20]:

$$H_{chain} = -\epsilon_j \sum_j c_j^\dagger c_j + \sum_{j=0}^{N-1} \left[-\tau\left(c_{j+1}^\dagger c_j + c_j^\dagger c_{j+1}\right)\right] + \sum_{j=0}^{N-1} \left[|\Delta|\left(c_j c_{j+1} + c_{j+1}^\dagger c_j^\dagger\right)\right]$$

Equation 1: Hamiltonian of Kitaev Chain. ϵ is the On-site energy parameter, τ is the Hopping energy parameter, Δ is the Superconducting parameter, j is the site number.

It is divided into 3 different parts, each reflecting one part of the Kitaev Chain model, each with its own energy parameter:

- The first part of the Hamiltonian $\left(-\epsilon_j \sum_j c_j^\dagger c_j\right)$ represents the occupied sites of the system. *On-site energy* parameter (ϵ_j) multiplying it represents the energy of the site filled by a fermion.
- The second part of the Hamiltonian $\left(\sum_{j=0}^{N-1} -\tau\left(c_{j+1}^\dagger c_j + c_j^\dagger c_{j+1}\right)\right)$ represents the tunneling interactions in-between sites that allow the movement of fermions. The energy parameter is the *Hopping energy* (τ),

which is the energy for one particle o move from one site to the other (or for it to be created in one site and destroyed on the other).

- The third part of the Hamiltonian $\left(\sum_{j=0}^{N-1}|\Delta|\left(c_j c_{j+1} + c_{j+1}^{\dagger} c_j^{\dagger}\right)\right)$ represents the energy of breaking the cooper pair that come from the superconductor substrate into the Majorana Wire. The parameter for this energy is *Superconductor energy* Δ, also called *Delta parameter*.

1.4. Model

Using the Hamiltonian for the Kitaev Chain presented that uses the Second Quantization Formalism, we can represent all the potential energy-states of a system in graphical form by using a Hamiltonian Matrix followed by the representation of the possible states of the system in a vertical column. As with the operator matrix (**Representation 7**), the position of energy parameters within the Matrix represents not only the energy of the system in the original state but the energy to make interactions between states. For example, the following is the energy matrix for 2 sites Kitaev Chain:

$$\begin{pmatrix} 0 & 0 & 0 & \Delta \\ 0 & \epsilon_1 & \tau_{1,2} & 0 \\ 0 & \tau_{1,2} & \epsilon_2 & 0 \\ \Delta & 0 & 0 & \epsilon_1 + \epsilon_2 \end{pmatrix} \begin{matrix} |0,0> \\ |1,0> \\ |0,1> \\ |1,1> \end{matrix}$$

Representation 8: Representation of the Hamiltonian of a 2 site Kitaev Chain system. ϵ_j is the On-site energy of the site j, $\tau_{k,l}$ is the Hopping parameter between a specific combination of neighboring sites k and l, and Δ the Superconducting parameter.

As with the operator matrix before, each cell position represents its connection between the original state (the row) and another state (the column). The original state of the row is already at the end of the row (|1,0>), and the state in which a cell is interacting is the column number of the cell. For example, the first cell in the 4th row is

originally in the fourth state (|1,1>) interacting with the first state (|0,0>). If the cell is filled with a 0, it means that this interaction is not possible.

So, for example, taking the second row of the Hamiltonian matrix we have the following values:

$$(0 \quad \epsilon_1 \quad \tau_{1,2} \quad 0)|1,0>$$

Representation 9: Eigenenergy of the second state of a two sites Kitaev Chain. ϵ_j is the On-site energy of the site j, $\tau_{k,l}$ is the Hopping parameter between a specific combination of neighboring sites k and l.

The first cell is the interaction between the second and first states of the system, which is invalid. The second cell, which is in the second column, is the energy of the system without interactions, and naturally is the energy of just filled site. The third cell is the energy for the fermion filling the second site to hope between the first and second site of the system, therefore making an interaction between the two states. The fourth cell is the interaction between the second and fourth states, and this interaction is invalid.

This representation of the Hamiltonian is very useful not only to observe the difference in the eigenenergy of the states in the system but also to make calculations, like solving the Schrödinger Equation to find the probability of finding a fermion in any site of the system. To do these calculations, the Hamiltonian Matrix needs to be broken into different blocks based on its pairing. Independently of how long is a Kitaev Chain, the system can have only two parities, depending on the number of fermions within the system. The blocking of the Hamiltonian Matrix by parity will include only the cells that deal with states of such parity interacting with states with the same parity. The two energy block matrixes created from the two sites system are, by parity:

$$Even \rightarrow \begin{pmatrix} 0 & \Delta \\ \Delta & \epsilon_1 + \epsilon_2 \end{pmatrix} \begin{matrix} |0,0> \\ |1,1> \end{matrix}$$

$$Odd \rightarrow \begin{pmatrix} \epsilon_1 & \tau_{1,2} \\ \tau_{1,2} & \epsilon_2 \end{pmatrix} \begin{matrix} |1,0> \\ |0,1> \end{matrix}$$

Representation 10: The energy blocks of Even and Odd parity, respectively, taken from the Hamiltonian of the full system.

Each of the energy blocks represents the energetic results by parity, and each of those can further be divided into two different eigenstates: ground or excited. These vary depending on the interactions of each of the forming states, according to the following equations:

$$Even\ ground\ state \rightarrow |e> = \frac{1}{\sqrt{2}} * (|0,0> - |1,1>)$$
$$Even\ excited\ state \rightarrow |e'> = \frac{1}{\sqrt{2}} * (|0,0> + |1,1>)$$
$$Odd\ ground\ state \rightarrow |o> = \frac{1}{\sqrt{2}} * (|1,0> - |0,1>)$$
$$Odd\ excited\ state \rightarrow |o'> = \frac{1}{\sqrt{2}} * (|1,0> + |0,1>)$$

Equation 2: The eigenenergy of Even and Odd parity, in ground and excited stated.

This will serve as the mathematical foundation for the representation of the physical system of the Majorana Wire, allowing us to make analytical analyzes of the system, and allowing to perform numerical analyzes and predict real results. These will be done by inputting numerical values to the parameters in the Hamiltonian to represent different regimes the system might be, allowing to explore multiple possibilities of how to work with the Majorana wire. There are many different possible regimes, so one must be chosen that allows and facilitates the control of the MZM's on the ends of the wire.

There is, however, only one controlled regime that allows the creation of the MZM's at the end of the wires: the *Ideal Kitaev Limit*. This is a specific regime that

calls a specific value for all the parameters within the system, and while its name is "Ideal" it is perfectly achievable within reality. It requires the system to be in a dimerized state and have the following values for its energy parameters:

- All sites within the system have their On-site energy equal to 0 ($\epsilon_j = 0$, for any *j*).
- Hopping and Superconducting parameters within the system are both equal to one another and equal to 1 ($\tau_j = 1 = \Delta$, for any *j*).

With this great foundation for the simulations of the Majorana Wire we can begin calculations to observe the workings of the system. As this system would create MZM's as wanted, the focus of this research would be to find results that are energetically different, allowing for easy readings of the parity of the system.

2. Numerical Work

2.1. Numerical Work and Quantum Dot

Using the Ideal Kitaev Limit models in the simulations, interesting results were possible to be established. By solving the Schrodinger equation showed that the system at ground state forms a two-fold degeneracy, and both parities show the same energy level. This is positive, given that this degeneracy allows the system to easily flip to any state and creates a non-preferential nature to either state, which makes the system an ideal qubit, but this also creates the problem that it cannot be differentiate energetically. With that, direct measurements of the system parity are impossible, but it is still possible to try to measure the system parity indirectly by connecting a quantum dot to the system, as it can be seen

The quantum dot connection to the system allows a new site for the system, which does not need to have the same parameters and the Ideal Kitaev Limit, allowing the fermions within the chain to interact with it in unique ways. The quantum dot would be connected to both ends of the system, limiting the interactions of sites of the system from only the sites at the ends of the system, and the two connections to the dot would allow two different possible tunnelings from which fermions from the system interact with the quantum dot. The parameters that interact with the quantum dot don't need to follow the regime of the Ideal Kitaev Limit, which means that their values can be different from the others, and this allows some control over the interactions between the Kitaev Chain and the quantum dot, and this control can be used to select and identify the parity.

By controlling the tunneling parameter between the quantum dot and the Kitaev chain it is possible to control the interactions of fermions from the Kitaev Chain to the quantum dot, allowing to control what conditions have a better probability to end with the quantum dot filled. By tunning the parameter in a certain way, it is possible to create conditions in which it is possible to make sure that if the quantum dot is filled the system is a certain parity, allowing to infer the parity of the system through the state of the quantum dot. This is a system for parity-to-charge conversion, where the parity of the system can be inferred by the charge of the quantum dot and is an indirect measurement of the parity of the Kitaev Chain.

Naturally, the addition of the quantum dot onto the Kitave Chain alters the Hamiltonian of the entire system, which is the sum of the Hamiltonian of the Kitaev Chain and the Hamiltonian of the Quantum dot and the interaction between them. The total Hamiltonian of the system (H) is then a sum of the Hamiltonian of the chain (H_{chain}), which contains the energies of the sites in the chain and their interactions, and

the Hamiltonian of the dot (H_{dot}), which contain the energies of the dot and its interactions with the chain. They are latter is presented in **Equation 4.**

$$H = H_{chain} + H_{dot}$$

Equation 3: The Hamiltonian equation for the Kitaev Chain in addition to the quantum dot.

$$H_{dot} = -\epsilon_{dot} c_{dot}^{\dagger} c_{dot} - \tau_{dot}\left[\left(c_1^{\dagger} c_{dot} + c_{dot}^{\dagger} c_1\right) + \left(c_n^{\dagger} c_{dot} + c_{dot}^{\dagger} c_n\right)\right]$$

Equation 4: The Hamiltonian equation of the Quantum dot and its interaction to the Kitaev Chain.

The addition of the quantum dot also affects how the system will be represented. The addition of a quantum dot to the Kitaev chain effectively means an increase in the size of the chain in 1, although there are many differences, and we can still use the Second Quantization formalism to represent the entire system. As the quantum dot can only be either filled or not it can still be represented by a "1" or "0", respectively, and it will appear at the last position inside the *ket* utilized to represent the entire system state, separate from the state of the Kitaev Chain by a semicolon. As an example, the representation of a 2 sites system with a fermion on the first site and a filled quantum dot is the following:

$$|1,0;1\rangle$$

Representation 11: Representation of a 2 sites Kitaev Chain with the first site of the Kitaev chain and the quantum dot filled.

Although the representation of both different systems is seemingly similar, both the Second Quantization formalism and the Hamiltonian of any Kitaev Chain with a Quantum dot are different than just a Kitaev Chain with one more site. While the quantum dot can have the same parameters as the Ideal Kitaev Limit regime applies to the Kitaev Chain, it still isn't affected by the Superconductive parameter. The addition of the quantum site onto the Kitaev Chain also makes the system now have 8 different energy eigenstates, generated by a combination of 3 different factors, that can be represented through Second Quantization formalism:

- The parity of the Kitaev chain, not including the fermions in the quantum dot. On the Second Quantization formalism, the even state appears as “e” and odd as “o”.
- The excitation level of the Kitaev Chain system. On the Second Quantization formalism, the even state appears as “`” add to the parity of the system. For example, the excited even state is represented by “e`”.
- The filling of the quantum dot, using the usual method of representation of the filling in Second Quantization formalism.

For example, a system with a Kitaev Chain with an excited odd parity and a quantum filled dot would appear as:

$$|o`;1>$$

Representation 12: Representation of system with a Kitaev Chain with an odd parity and a filled quantum dot.

These 3 elements combine into 8 different energy eigenstates possible, which can be reorganized to form two different Hamiltonians considering the overall parity of the system (including the quantum dot). These two Hamiltonians are defined as the *Even Hamiltonian* (H_e) and the *Odd Hamiltonian* (H_o). These are shown in **Representation 13** and **14** with their specific eigenstates and shown again when taken into account the parameters of the Ideal Kitaev Limit regime at **Representation 15** and **16**.

$$\begin{matrix} |e;0> \\ |o;1> \\ |e';0> \\ |o';1> \end{matrix} \rightarrow H_e = \begin{pmatrix} -\Delta & \tau_{dot} & {}^{1}/_{2}\,(\epsilon_1+\epsilon_2) & 0 \\ \tau_{dot} & -\Delta+\epsilon_{dot} & \tau_{dot} & {}^{1}/_{2}\,(\epsilon_1-\epsilon_2) \\ {}^{1}/_{2}\,(\epsilon_1+\epsilon_2) & \tau_{dot} & \Delta & 0 \\ 0 & {}^{1}/_{2}\,(\epsilon_1-\epsilon_2) & 0 & \Delta+\epsilon_{dot} \end{pmatrix}$$

Representation 13: The block formed for the Hamiltonians of the Even Parity Kitaev Chain system with a quantum dot in its possible iterations.

$$\begin{matrix} |o;0> \\ |e;1> \\ |o';0> \\ |e';1> \end{matrix} \rightarrow H_o = \begin{pmatrix} -\Delta & 0 & {}^{1}/_{2}\,(\epsilon_1 - \epsilon_2) & 0 \\ 0 & -\Delta + \epsilon_{dot} & -\tau_{do} & {}^{1}/_{2}\,(\epsilon_1 + \epsilon_2) \\ {}^{1}/_{2}\,(\epsilon_1 - \epsilon_2) & -\tau_{dot} & \Delta & \tau_{dot} \\ 0 & {}^{1}/_{2}\,(\epsilon_1 + \epsilon_2) & \tau_{dot} & \Delta + \epsilon_{dot} \end{pmatrix}$$

Representation 14: The block formed for the Hamiltonians of the Odd Parity Kitaev Chain system with a quantum dot in its possible iterations.

$$H_e \rightarrow \begin{pmatrix} -\Delta & \tau_{dot} & 0 & 0 \\ \tau_{dot} & -\Delta + \epsilon_{dot} & \tau_{dot} & 0 \\ 0 & \tau_{dot} & \Delta & 0 \\ 0 & 0 & 0 & \Delta + \epsilon_{dot} \end{pmatrix}$$

Representation 15: The representation of the Hamiltonian of the Even parity taken into account the parameters of the Ideal Kitaev Limit regime.

Representation 16: The representation of the Hamiltonian of the Odd parity taken into account the parameters of the Ideal Kitaev Limit regime.

$$H_o \rightarrow \begin{pmatrix} -\Delta & 0 & 0 & 0 \\ 0 & -\Delta + \epsilon_{dot} & -\tau_{dot} & 0 \\ 0 & -\tau_{dot} & \Delta & \tau_{dot} \\ 0 & 0 & \tau_{dot} & \Delta + \epsilon_{dot} \end{pmatrix}$$

2.2. Measuring the Quantum dot

The **Representations 15** to **16** represent the Hamiltonians of a Kitaev Chain with the addition of a quantum dot in the Ideal Kitaev Limit regime allow us to observe the development of the system. Using our understanding of how the cells within the matrix related to the original and final state of the system, it is possible to make some predictions of how it will behave in the simulations given their different starting points, especially considering our desired results.

Given all of this, let's consider that the system starts in the ground state, independently if it has an odd or even parity. In both cases, it would mean that the system would start at in one of the ground eigenstates of |e,0> or |o,0> and by Rabi oscillation there can be an interaction with the quantum dot so the system eigenstates changes to |o,1> or |e,1>, in respect to the parity of the original eigenstate. This will happen because the tunneling between the Kitaev Chain and the quantum dot (τ_{dot}) can

be activated, making this a switch that can be turned on for chosen amounts of time. The switch must stay on for a specific duration, a single "pulse", to properly capture the fermion when it tunnels to the quantum dot, but not allow it to tunnel back to the Kitaev Chain. The best value for such will vary with the strength of the pulse, that is, the value for the τ_{dot} parameter.

This means that any system will have, before the switch is turned on, the τ_{dot} value set to 0, disallowing any transition to the states where the quantum is filled. But, as the switch is turned on, the τ_{dot} is the value changes to the *pulse strength* (τ_{max}) instantaneously and is kept at this value for the *pulse duration* (T), when the switch is turned off and the value returns to 0, also instantaneously. This instantaneity is fundamental for the system, as it is necessary to avoid any irregularities on the system and to guarantee that the system has two clearly defined states, that is with the switch on or off. This is represented by **Equation 5**, which shows a time equation that relates the pulse strength to pulse duration in a step function, and with this in mind, we can better analyze the two Hamiltonians presented in **Representations 15** and **16.**

$$\tau_d(t) = \tau_{max}\Theta(\mathrm{t})\Theta(\mathrm{T}-\mathrm{t})$$

Equation 5: Function of the pulse of the value of the pulse strength. τ_{max} is the maximum value of τ_{dot}, T is the pulse duration and t is the current time.

In the Hamiltonian for the Even parity (H_e, **Representation 15**) the system starts energetically starts at |e,0> and can interact to |o,1> because of tunneling coupling with the quantum dot. Given that their final state has the on-site energy for the quantum dot (ϵ_{dot}), it means that the quantum dot would be filled by a fermion, and therefore the parity of the system could be inferred by measuring its charge. But the Hamiltonian for the Odd parity (H_o, **Representation 16**) is different.

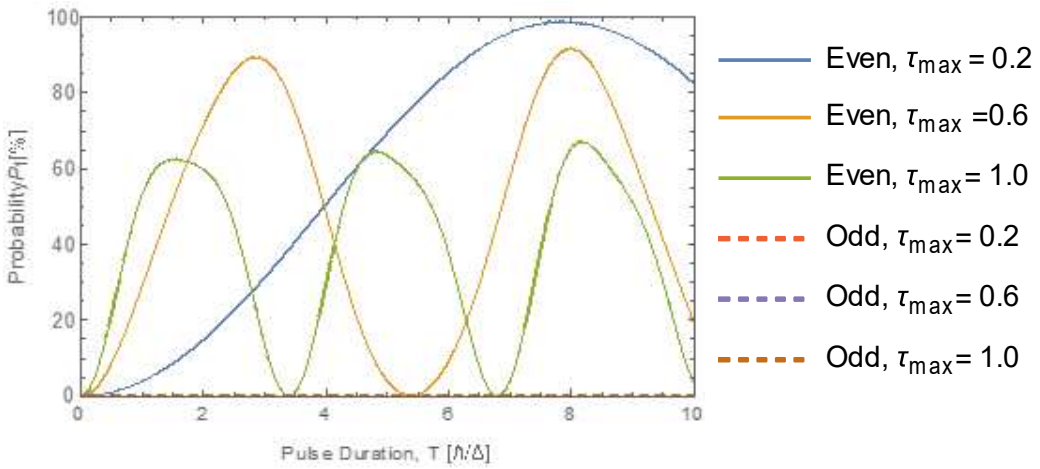

Graph 1: Probability curves for the quantum dot to be find filled for different Pulse Strengths for the Hopping parameter, in a system with Even and Odd parity.

While its original and final energy levels are the same (as expected from a twofold degenerated state), the value on the second cell of the first row is empty, that is, has just a "0". This means that this change of state is invalid, and therefore cannot happen, which means that a system starting on the conditions giving in **Representation 16** will never end with the quantum dot filled. This effect can be seen in simulations to solve the Schrodinger equation on the quantum dot site on **Graph 1**, showing the probability to find the quantum dot filled in relation to the pulse duration for a few different pulse strengths.

Graph 1 shows the probability curve of the system for Even parity, and it is easy to see that each different value of Pulse Strength creates a different curve, with different periods and maxima. These will correspond to the Rabi Oscillation into the quantum dot site, and its period can be mathematically compared with the expected Rabi period calculated from the Even Hamiltonian of the system in **Representation 16**. To do so we focus on the first quadrant of the Matrix, the ground state block, formed by a 2x2 matrix of the cells in the upper left corner of the Hamiltonian, and all calculated periods match with the observed Probabilities curves periods. From this ground state

block is also possible to verify if the parity of the system can be discovered through the electron density of the system, but both parities show the same density.

After calculating the Rabi Frequency equation (**Formula 1**), it is possible to calculate the Rabi Period and compare the period to the period found on the resulting simulations we produced. The results of this can be seen in **Table 1**, which shows the different periods found for different Pulse Strengths on the simulated results and the calculated Rabi Frequency. It can be seen the values to be very close, helping to verify that these simulations are working properly and representing correctly the expected behavior of this system in different parameters. The Difference increases as the Pulse Strengths grows, but it is because the period decreases quickly as the Pulse Strength increase, so even if the difference stays less than 0.3 ħ/Δ in all values, the relative value of this difference increases.

$$Rabi\ Frequency = \frac{\tau_{dot}}{\hbar * \pi}\ [\Delta/\hbar]$$

Formula 1: Calculated Rabi Frequency for the system from its ground state within the regime of the Ideal Kitaev Limit

Pulse Strength [Δ]	Rabi Period (analytical), (T_{Rabi}) [ħ/Δ]	Rabi Period (numerical), (T_{Rabi}) [ħ/Δ]	Difference [%]
0.2	15.71	15.76	0.3%
0.4	7.85	7.96	1.4%
0.6	5.24	5.41	3.1%
0.8	3.93	4.14	5.1%
1.0	3.14	3.39	7.4%

Table 1: Periods of the simulated results and frenquency of the calculated Rabi Oscilation for the ground state system following the regime of the Ideal Kitev Limit (**Formula 1**).

While the results for the quantum Even Hamiltonian are visible and show a different probability curve for each value of pulse strength, as is expected, the values

for the Odd Hamiltonian are all the same at the bottom of the graph. As expected, independently of the pulse strength, there is no probability of finding the quantum dot filled if the system has an Odd parity. This could signify that, if there is a detectable charge within the quantum dot at the end of the defined pulse duration, we could already infer that the system is in Even parity, as Odd parity systems can't fill this dot. Unhappily this is only true in the most ideal of cases because even the Even Probability curve has a chance of failing in filling the quantum dot. This chance can be seen in the Probability Curve as the distance between the maximum and the 100% Probability (the top frame of the graph).

The Even parity probability curves shown in **Graph 1** shows some differences, sometimes sizeable, to the possible maximum of probability. This difference is called *Parity Readout Error* (ϵ), and effectively means that, while the system is Even, there is a chance that the quantum dot will be unfilled, which creates a degree of unreliability to the system. This can be caused by 3 main factors[19]:

- **Leakage due to strong readout tunnel pulse:** The tunnel pulse between the Kitaev chain and the quantum dot induces a transition of the energy states in the Kitaev chain, which can then interact between finite-energy levels. It happens strongly in higher τ_{max}.
- **Incomplete charge Rabi oscillations due to slow charge noise:** It happens when electronic noise detunes the quantum dot so the Rabi oscillations are only partial. Naturally, this affects the filling of the quantum dot, which may cause a misreading of the parity of the system. It is more prevalent at weaker τ_{max}.
- **Charge relaxation to photon emission:** Although working in close to zero temperatures the system is still able to randomly emit a photon to

go to a lower energy state. In a system with even parity, the system can be either excited or ground energy. When the system de-excites, it can also alter the system parities to one of the other possible[19].

Although the parity readout error cannot be fully eliminated, a careful tunning of parameters and conditions should allow the value to become so small to be virtually negligible and therefore not an issue for future works. Ideally, the system should have high reliability but lower pulse duration, maximizing the number of possible pulses in any finite amount of time and subsequently the efficiency of the system.

As it can be seen in **Graph 1** the reliability of the system increases seen to increase with the use of smaller pulse strengths, mostly due to reduction in the leakage of the system, but also start to require considerably longer pulse durations. From now on this work focuses on varying different parameters and trying different approaches to try to identify the best parameters to find the best results possible for the system.

2.3. Mathematical Analysis

Being possible to simulate different iterations of the system with different parameters, it is possible to evaluate these different simulations in relation to different factors, especially the values of the parity readout error and the pulse duration. These multiple iterations will each have their own probabilities curves, and analyzing them will help to understand how the system develops in different conditions. One of the best ways to analyze these results is to develop analytical formulas to better understand and mathematically analyze, the development of the system on changing conditions.

To make on of such analyzes, we first took the system as described before (Kitaev chain in the Ideal Kitaev Limit with a quantum dot connected to the ends of the chain with the variable value of the tunneling to the dot and on/site energy) and define

what are the variables that we are most interested in. We choose three variables, two parameters for the system and on a result from the system, which the values, and their interactions, are of particular interest to us: Parity Readout Error (ϵ), Pulse Duration (T), and Pulse Strength (τ_{max}). Pulse Duration, in the case of the analyzed data, is the duration of the pulse necessary to get maximums in the Probability Curves of a given Pulse Strength.

Of the three, the one that "guides" the system the most is the Pulse Strength, which will define the Probability Curve format, and therefore the maximum in these and the values of Parity Readout Error, and by progressively increasing it we can observe how this change affects the other two variables. By varying it from 0 Δ to 1 Δ we produced **Graphs 2 (a)** and **(b)**, and by fitting a curve to its data we were able to generate fitting formulas. These are important not only to better understand, and help to model, the behavior of future calculations, but they allow us to compare the results produced by these simulations and the analytical results obtained in the literature to

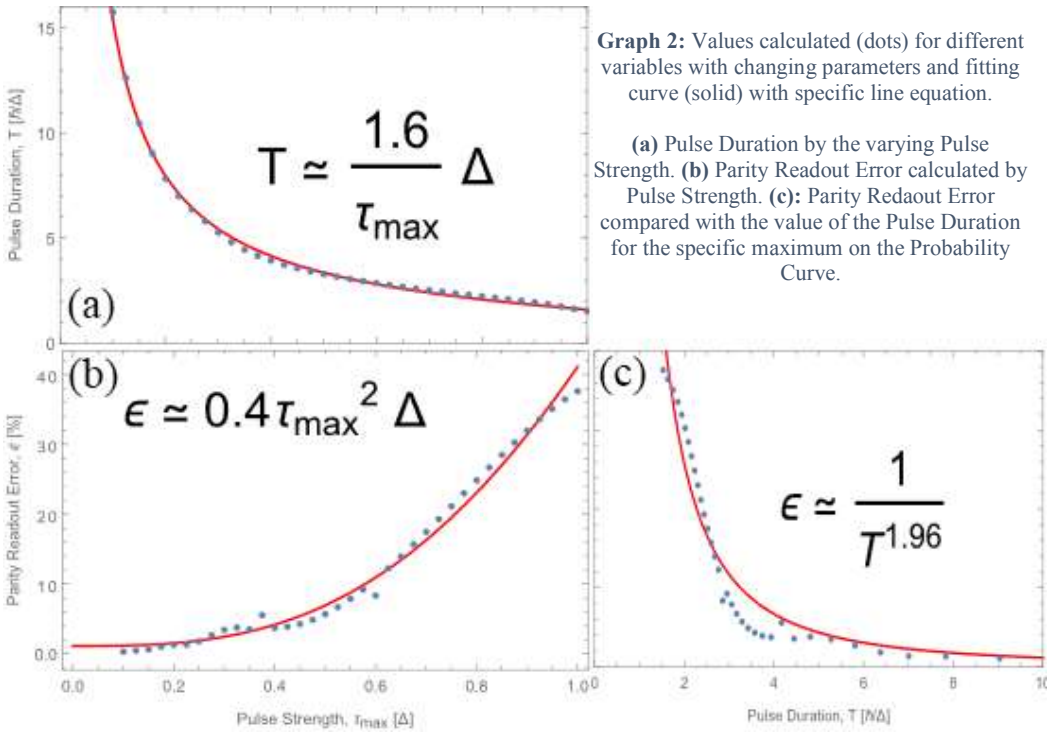

Graph 2: Values calculated (dots) for different variables with changing parameters and fitting curve (solid) with specific line equation.

(a) Pulse Duration by the varying Pulse Strength. **(b)** Parity Readout Error calculated by Pulse Strength. **(c):** Parity Redaout Error compared with the value of the Pulse Duration for the specific maximum on the Probability Curve.

verify the correctness of our simulations. It was also possible to create **Graph 2 (c)** that compares the change in the Parity Readout Error as the Pulse Duration changes.

All the formulas and graphs which are presented come from the Even parity systems, as simulations made for the system in odd parity gave the same result without variation that fits with the fact that the Odd parity systems have no probability of filling the quantum dot.

Using these Pulse Duration values it is possible to calculate the different Parity Readout Errors in different Pulse Strengths, focusing on the Pulse Duration that gives the first maximum in the Probability curve. As it can be seen in **Graph 2 (c)**, the Parity Readout Error we focus on is at the maximum of the Probability Curve, as if we would use this Pulse Strength, we would only focus on the best value to find the Quantum dot filled. The different values of Parity Readout Error for different Pulse Strengths, and how their Pulse Durations values vary, can be seen in **Graphs 2 (a)** and **(b)**, respectively.

These results already give us some idea of how the system will behave in future simulations, and the trends fit with the literature[19]: the smaller the Pulse Strength, the lower the Parity Readout Error, and the higher the Pulse Duration. This creates an unideal situation, where to increase the confidence in the system it is necessary to decrease the efficiency of the same system as it takes longer to do a measuring. There is, however, more that can be done with the system that can be worked to try to counterbalance it.

2.4. Changing the Quantum Dot On-Site Energy

All sites within the system, be on the Kitaev Chain or in the quantum dot, will have an on-site energy, which will be the energy added to the system whenever a

fermion fills this site. In the system, however, there will be two different types of sites, which will vary in the value of the on-site energy. The first kind of sites are those which are within the Kitaev Chain that, according to the Ideal Kitaev Limit, have a value of 0 on the on-site energy and must stay so. The other kind is the only site on the quantum dot, which value is not fix. So far, we have worked with the value for the on-site energy on the quantum dot to be the same as the value for the sites in the Kitaev Chain, which is 0, but in this Section we will vary its value.

This variation, however, will be very small. The values that the on-site energy can assume to keep with the consistency of the system presented so far are very small, lower than 0.01 Δ, so the effects on the Probability Curve are very small, as presented in **Graph 3**. After multiple calculations with On-site energies for the quantum dot varying from 0.001 to 0.01, the difference caused by the presence of this on-site energy was never more than 0.2% at the highest value of on-site energy, and to the smaller values being about a magnitude lower. These differences, however, were always

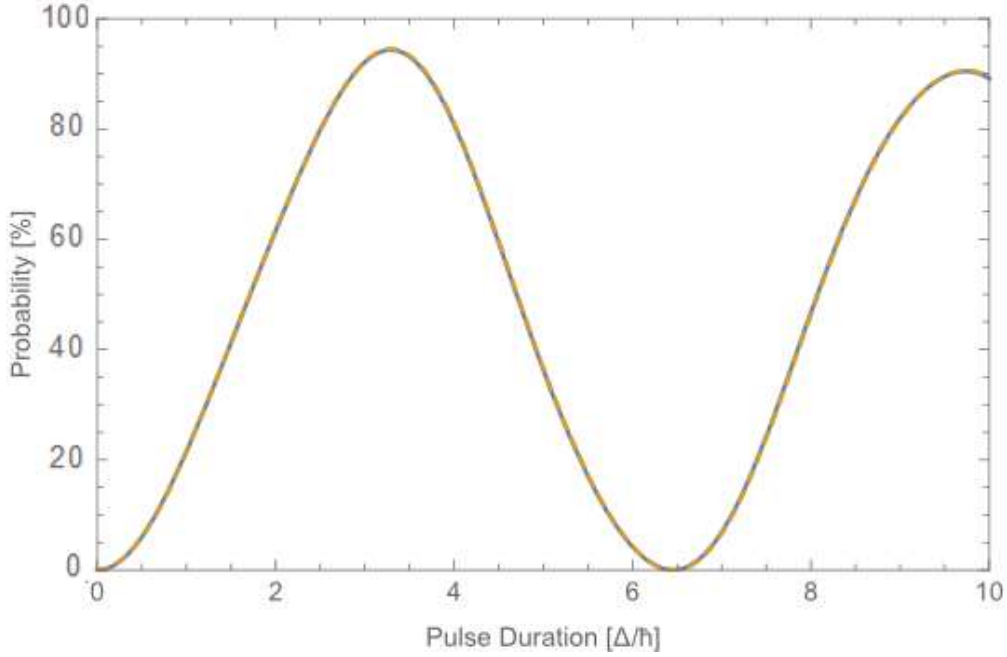

Graph 3: Two Probability Curves for a Even parity system with Pulse Strength of 0.5 Δ, but with different On-site energy for the quantum dot. The blue solid line has an On-Site energy for the quantum dot of 0 Δ, and the dashed orange line has 0.01 Δ. The difference is so small, it is barely noticeable.

beneficial to the Probability Curve. Similar effects in value were also perceptible on the Pulse Duration of the maxima of these Probability Curves, where the Pulse Duration was also affected by, at the highest of On-site energy values, 0.4%. This difference was more pronounced at high Tunneling values, as these had smaller Pulse Duration, and considerably less pronounced at lower values, sometimes with 2 orders of magnitude lower. Different from the differences in the maxima of the Probability Curves, this difference was detrimental to the Pulse Duration, increasing it instead of reducing it.

The results found through these calculations, as it was done before, can be verified by the calculation of the Rabi Frequency calculated for the specific Hamiltonian. This frequency is different from the previously used, as it requires the addition of the On-Site Energy of the quantum dot (ϵ_{dot}) term as well as the On-site energy to the quantum dot, variation which creates **Formula 2**. After these additions, however, the resulting periods keep the same similarity with the simulated results, once again helping to verify our simulations. The results found can be seen in **Table 2**, which shows a slight increase in the difference between the simulated and calculated periods.

$$Rabi\ Frequency = \frac{\sqrt{{\tau_{dot}}^2 + \frac{{\epsilon_{dot}}^2}{4}}}{\hbar * \pi}\ [\Delta/\hbar]$$

Formula 2: Calculated Rabi Oscilation for the ground state system following the Ideal Kitaev Limit regime with added On-Site Energy of the quantum dot.

This is due to the dampening effect caused by the addition of the On-site Energy of the quantum dot, which not only reduces the amplitude of the curves but also it's period. As long as the values of the On-site Energy of the quantum dot are kept small (within the pre-established limit of 0.01 Δ) and we abstain from going beyond Pulse Strengths of 1 Δ, then the difference is expected to be small.

Pulse Strength [Δ]	Rabi Period (analytical), [ħ/Δ]	Rabi Period (numerical) [ħ/Δ]	Difference [%]
0.2	15.70	15.77	0.4
0.4	7.85	7.98	1.6
0.6	5.24	5.43	3.6
0.8	3.93	4.15	5.7
1.0	3.14	3.40	8.2

Table 2: Periods of the simulated results and frenquency of the calculated Rabi Oscilation for the ground state system following the regime of the Ideal Kitev Limit with the addition of the On-site Energy of the quantum dot (**Formula 2**).

2.5. Hopping Parameter with Multiple Pulse Strengths

In the system, no variable of the Kitaev Chain can be changed while it remains in the Ideal Kitaev Limit regime, and it must remain in this regime to generate the MZMs at its ends. This leaves that the only variables which can be changed in the system are those related to the quantum dot, more specifically, the on-site energy and the tunneling energy of the quantum dot, and in the previous sections we already showed different possibilities for such variations in the system. This, however, does not mean that there are no other ways to alter the system.

Paying attention to **Figure 2** it is possible to see that each end of the Kitaev chain is connected to the quantum dot, for a total of two different lines, each line representing tunneling to one end to the Kitaev Chain. So far, we have controlled the value of both the tunneling as if they are equal at all moments, but there is no reason that this must be the case. It is possible to consider that each tunneling has a different Pulse Strength, although both still work in a switch system (0 when off, Pulse Strength when on) and are turned on/off at the same time. This is represented in **Figure 3**.

This doesn't fundamentally alter the system but creates a cascade effect starting at the Hamiltonians of the Kitaev Chain plus the quantum dot. Imagining this Hamiltonian, and taking into account the effects of the Ideal Kitaev Limit regime, we have the results found on **Representation 13** and **14** for the Even and Odd Hamiltonians for the system, respectively.

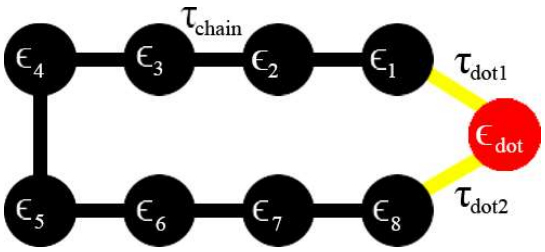

Figure 3: Representation of the Kitaev Chain with 8 sites and an added quantum dot to both its ends, each end with a different Hopping parameter. If the Kitaev chain is on the Ideal Kitaev Limit ϵ_1 to ϵ_8 are 0 Δ, and all tunneling between sites within the chain are equal to τ_{chain} = 1 Δ.

Interestingly, these representations now show values for values at position (2,2) and (1,2) in the Odd Parity Hamiltonians, which mean that the system could be able to change state. These values also explain why they were not there before, as their values $\left(\frac{-\tau_{dot1}+\tau_{dot2}}{2}\right)$ would become 0 if $\tau_{dot} = \tau_{dot2}$, which is exactly what was happening beforehand when we consider both connections with the same Hopping parameter. With this difference, it is expected that the Odd Parity system will show some probability of having filled the quantum dot, and therefore appearing as probability curves on graphs.

This is shown to be true on the result of simulations shown on **Graph 5** and **8**, that show multiple graphs containing 5 different combinations of Pulse Strengths for τ_{dot1} and τ_{dot2}, which allows us to analyze the behavior of the probability curve under different values of Pulse Strength Obviously, the curve in each graph in which both Pulse Strengths are the same is the same result as the one that would be found using the previous model.

$$H_e \rightarrow \begin{pmatrix} -\Delta & \frac{\tau_{dot} + \tau_{dot2}}{2} & 0 & 0 \\ \frac{\tau_{dot} + \tau_{dot2}}{2} & -\Delta + \epsilon_{dot} & \frac{\tau_{dot1} + \tau_{dot2}}{2} & 0 \\ 0 & \frac{\tau_{dot1} + \tau_{dot2}}{2} & \Delta & 0 \\ 0 & 0 & 0 & \Delta + \epsilon_{dot} \end{pmatrix}$$

$$H_o \rightarrow \begin{pmatrix} -\Delta & \frac{-\tau_{dot1} + \tau_{dot}}{2} & 0 & \frac{\tau_{dot1} - \tau_{dot2}}{2} \\ \frac{-\tau_{dot1} + \tau_{dot2}}{2} & -\Delta + \epsilon_{dot} & \frac{\tau_{dot1} + \tau_{dot2}}{2} & 0 \\ 0 & \frac{\tau_{dot1} + \tau_{dot}}{2} & \Delta & \frac{-\tau_{dot1} - \tau_{dot}}{2} \\ \frac{\tau_{dot1} + \tau_{dot}}{2} & 0 & \frac{-\tau_{dot1} - \tau_{dot2}}{2} & \Delta + \epsilon_{dot} \end{pmatrix}$$

Representation 13 and 14: The block formed for the Hamiltonians of the Even and Odd Parity, respectively, Kitaev Chain system with a quantum dot in its possible iterations with different values for each connection to the quantum dot.

Comparing **Graph 4** to **Graph 1**, which also shows different probability curves for Even parity systems, it is possible to see that there is a positive difference in all graphs. While before it could be seen that curves with low Pulse Strength showed good Parity Readout Error, they also showed long Pulse Duration, and curves with high Pulse Strength showed good Pulse Durations but bad Parity Readout Errors. In **Graph 4** it is possible to see that some results in all combinations of values for the τ_{dot1} and τ_{dot2} curves showed small Pulse Duration while having good Parity Readout Errors. We can't, however, consider the Parity Readout Error of the system just by analyzing the possibilities of one of the parities, and both must be taken into consideration.

This doesn't happen with all curves, however, and the reason that it happens to some and not others can be perceived when paying attention to the values of the combination and the resulting Hopping Parameter of the system. The Hopping parameter for a system in any combination is given by following the formula presented

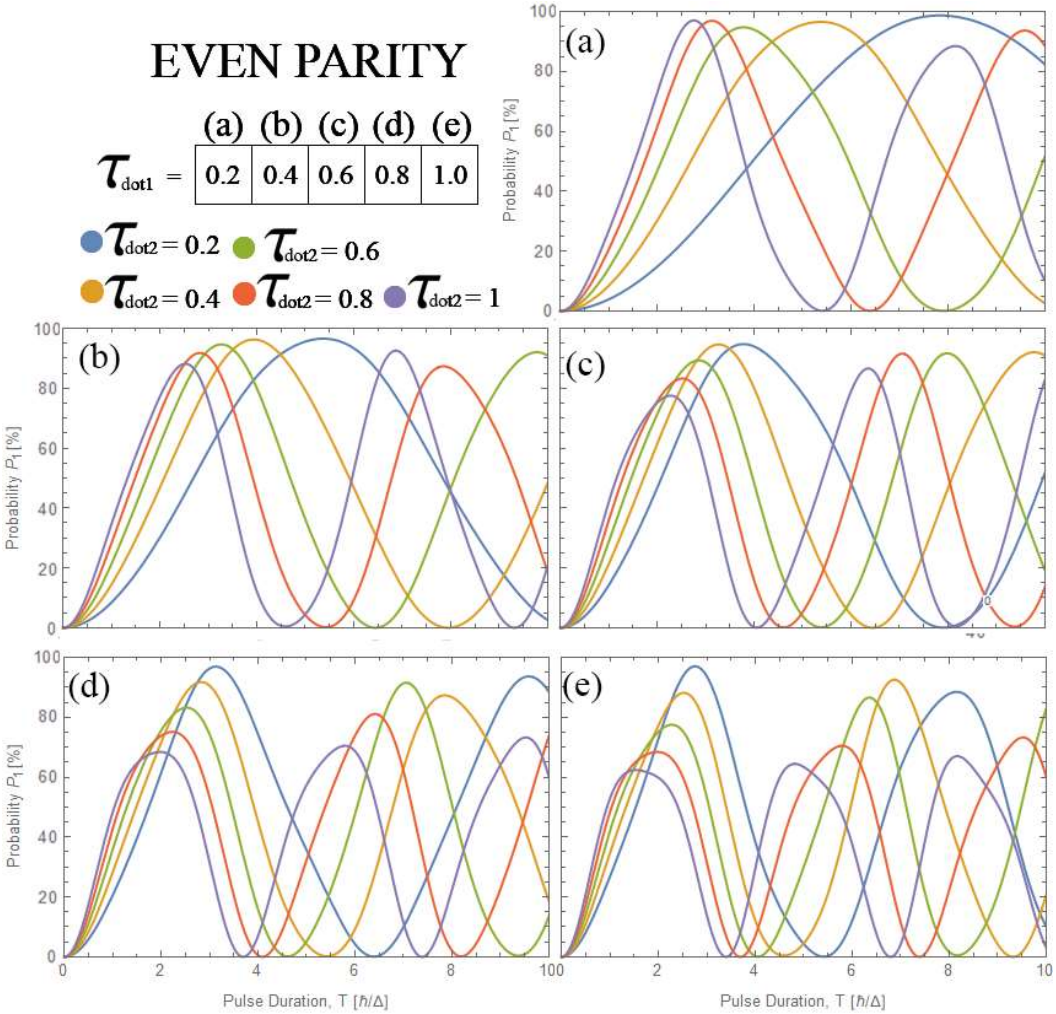

Graph 4: Probability of finding the quantum dot filled in for different combinations of τ_{dot1} and τ_{dot2} in a system with an Even parity. The on-site energy for the quantum dot is 0.

in the position (2,2) in the energy Hamiltonian, which represents the change of state of the system from the Kitaev Chain in a certain parity to it changing parity but filling the quantum dot. Each different parity has a different Hopping Parameter, and the formulas for the even and the odd parity are presented as **Formulas 1** and **2**, respectively.

$$\tau_{dot} = \frac{\tau_{dot1} + \tau_{dot2}}{2} \ [\Delta]$$

Formula 3: Formula for the calculation of the Hopping parameter for the Even parity system with different Pulse Strength for each connection to the quantum dot.

$$\tau_{dot} = \frac{-\tau_{dot1} + \tau_{dot2}}{2} \ [\Delta]$$

Formula 4: Formula for the calculation of the Hopping parameter for the Odd parity system with different Pulse Strength for each connection to the quantum dot.

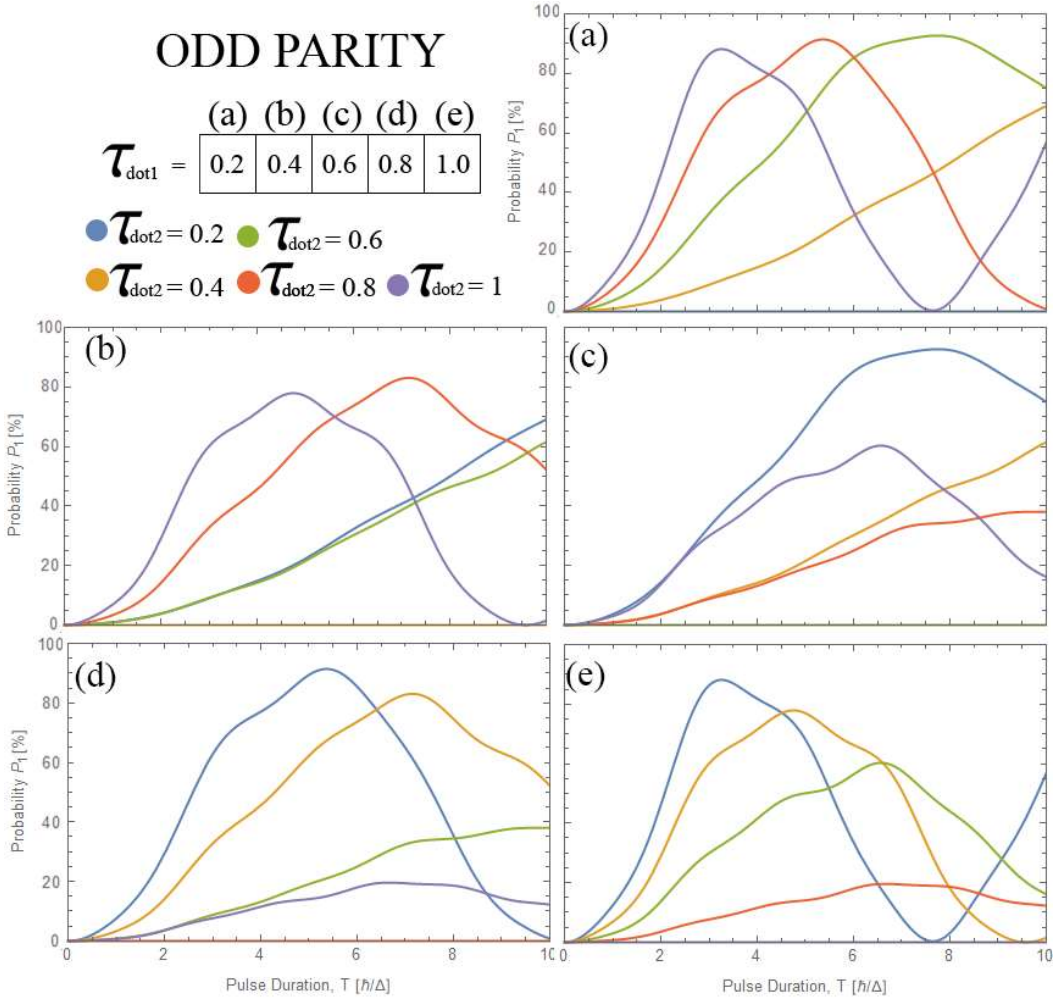

Graph 5: Probability of finding the quantum dot filled in for different combinations of τ_{dot1} and τ_{dot2} in a system with an Odd parity. The on-site energy for the quantum dot is 0.

These results can be seen in **Graph 5**, which show the probability curves for the Odd parity result with multiple combinations of τ_{dot} and τ_{dot2} values, including the combination of the same values. This combination, specifically, appears as a straight line at the bottom of the graph, as it follows the behavior presented before. It is also possible to see that the other lines while being very different from the synodal waves than the Even parity curves in **Graph 6** show a pattern to having longer Pulse Durations the closer that τ_{dot1} and τ_{dot2} values are to be the same.

As before, the simulated results are shown in **Graph 4** and **Graph 5** have been verified by comparing against the Rabi Frequency calculated for the system in its

ground state, but now with alterations to include the two different Hopping Parameters. Due to the existence of two different Hopping Parameters (**Formulas 3** and **4**), there is a need for two different Rabi Frequency formulas, one for parity. In both cases, it is only the τ_{dot} parameter that is changed from **Formula 1** (or **Formula 2**, if it is to consider the On-site Energy of the quantum dot too) that is substituted by the **Formula 3** or **4** if the system is in Even or Odd parity, respectively. Representations for both parities can be seen in **Formulas 5** and **6**.

$$Even\ Rabi\ Frequency = \frac{\sqrt{\frac{(\tau_{dot} + \tau_{dot2})^2 + \epsilon_{dot}{}^2}{4}}}{\hbar * \pi}\ [\Delta/\hbar]$$

Formula 5: Calculated Rabi Frequency for the ground state system following the Ideal Kitaev Limit regime with added On-Site Energy of the quantum dot and considering an Even Hopping Parameter (**Formula 3**) for different Pulse Strenghts.

$$Odd\ Rabi\ Frequency = \frac{\sqrt{\frac{(\tau_{dot2} - \tau_{dot1})^2 + \epsilon_{dot}{}^2}{4}}}{\hbar * \pi}\ [\Delta/\hbar]$$

Formula 6: Calculated Rabi Frequency for the ground state system following the Ideal Kitaev Limit regime with added On-Site Energy of the quantum dot and considering an Odd Hopping Parameter (**Formula 4**) for different Pulse Strenghts.

The simulation of the period of different combinations of Pulse Strengths has shown no significant Difference for the Even parity system, but it was noticed that this difference on Odd parity grows large when the parities are close and high. For this reason, our calculations have limited themselves to keep one of the Pulse Strength up to 0.5 Δ.

Beyond the Hopping Parameter, however, one more important factor to take into account a system with different Pulse Strength for different connections to the quantum dot. It is the fact that, because now the system in odd parity can fill the quantum dot the fact that the quantum dot is filled is no longer necessarily means that the system is in even parity. Beforehand an error in the readout would mean that the

quantum dot was not filled when the system was in even parity, but now the system might be in odd parity while the quantum dot is also filled.

This means that it is necessary to take into consideration both the Odd parity and Even parity probabilities before considering that a certain combination of Pulse Duration and Pulse Strength gives us a good result. A combination that has a 100% probability of having the quantum dot filled at one parity, but has also a 50% probability that it could be filled by a different parity has only 50% of being measured correctly. It is also important to mention that, as can be seen, whenever one of the values of Pulse Strength approaches 0 Δ, the probability curves for both parities become more and more similar, to the limit of becoming the same when one of them is 0 Δ. This effect can be seen in **Graph 6**.

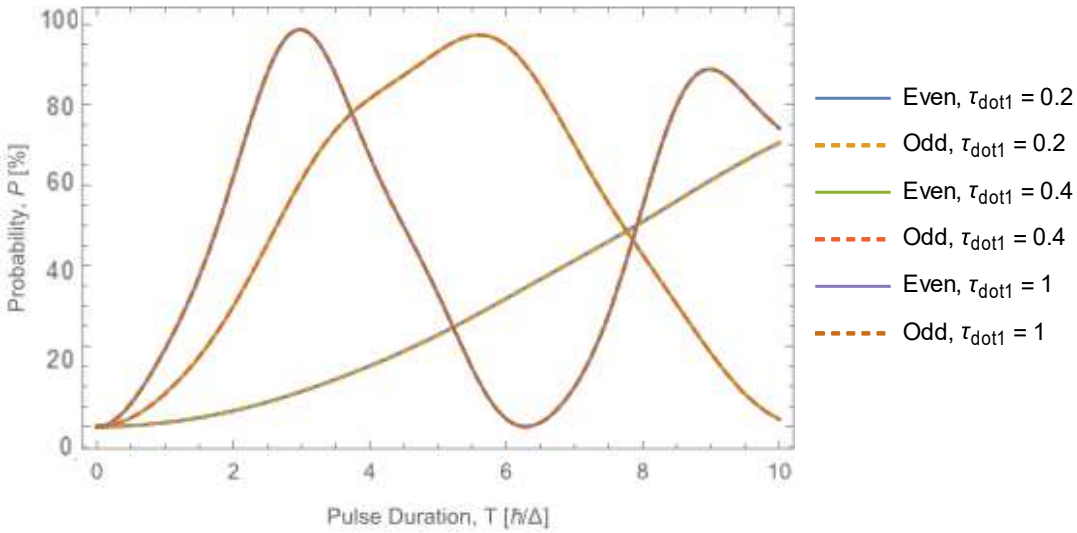

Graph 6: Probability of finding the quantum dot filled in for different of τ_{dot1} but all τ_{dot2} are equal to 0. Full lines are Even parity, dashed are Odd parity. The on-site energy for the quantum dot is 0.

3. Optimizing Parameters

3.1. Finding the best Hopping Parameter

In the previous section that the factor that affects the behavior of the probability curve is the Hopping Parameter, which varies for even and odd parities (**Formula 3** and

2, respectively). This value is produced by the combination of the Pulse Strengths, but this combination is seen to be more relevant to the Probability curve than the individual values of the Pulse Strengths. This allows us to investigate the system focusing on such combination, and after finding a promising combination to investigate and observe what would be the best fitting Pulse Strengths.

To observe such phenomena, we created simulations that will calculate the best value for the Parity Readout Error for certain combinations of Pulse Strengths. This best value is the smallest Parity Readout Error that the system can get, with the lowest Pulse Duration. Of the two Pulse Strength values, one was left to change progressively from 0 Δ to 1 Δ in 0.01 Δ steps while the other was kept fix at 0.5 Δ. For each step of the combinations, 5000 realizations were averaged, each with a randomly chosen on-site energy for the quantum dot attributed to it to take into account perturbation theory. These values were chosen from a random Gaussian variable with 0 Δ mean and 0.01 Δ noise, as it is presented in the literature[19].

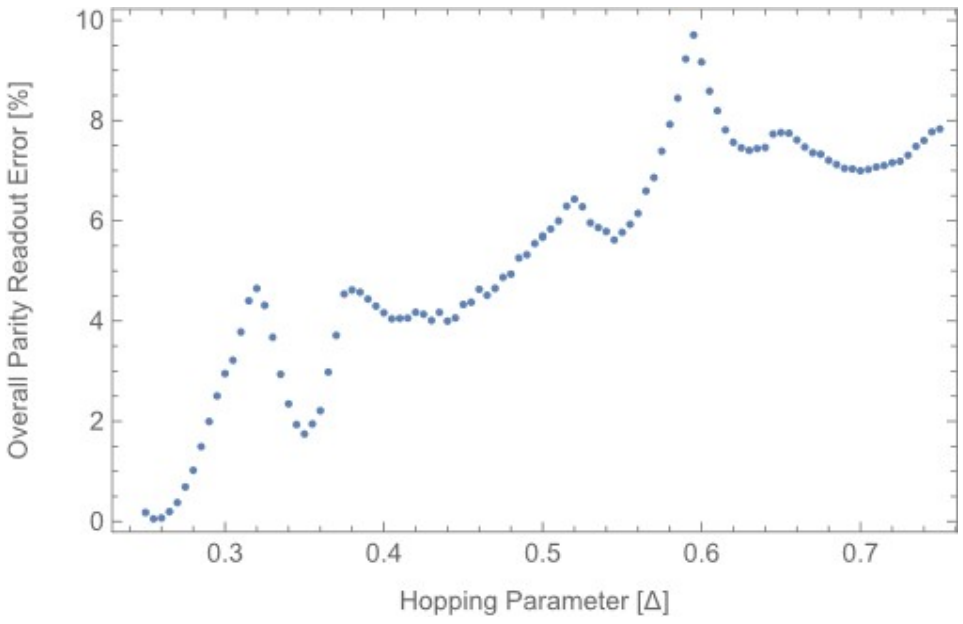

Graph 7: Best Parity Readout Error for the the Even system for different Hopping Parameters that vary from 0.25 to 0.75. The On-site energy of the quantum dot is defined randomly. The Hopping Parameter is calculated by the **Formula 3**.

For the Even parity system, this gives us middle range values of Hopping Parameters (calculated with **Formula 3**, the Even parity Hopping parameter formula), as the resulting combination of Pulse Strengths is just an average of the Pulse Strengths, and the combinations will vary from 0.25 Δ to 0.75 Δ. The values we obtained from the Parity Readout Error for the Even parity system can be seen in **Graph 7.** It can be seen that the values calculated for the Parity Readout Error are very small for the smallest values of the Hopping Parameters, with a semi-continuous increase until about 0.35 Δ, when it drops until about 0.43 Δ, from where it increases again. As one of the Pulse Strengths is fix at 0.5 Δ only the other one variate, and the interval of this drop goes from about 0.2 Δ to 0.36 Δ. While the Parity Readout Error results for the low combination are the best, it has been seen that low combination values also have a large Pulse Duration. For the Odd parity system, the Hopping Parameters that result from **Formula 4** (the odd parity Hopping parameter formula) go to the negatives, as **Formula 4** has a subtraction of the Pulse Strengths.

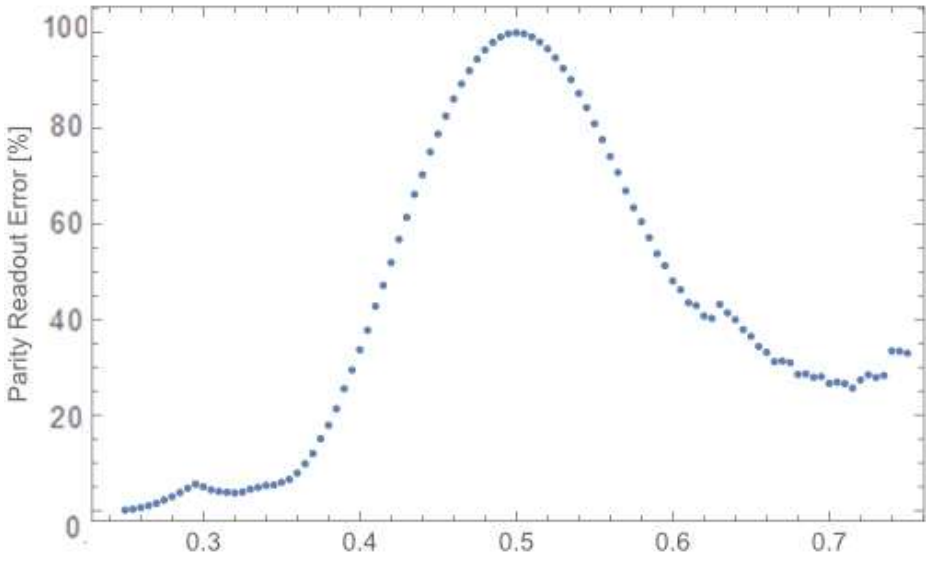

Graph 8: Best Parity Readout Error for the the Odd system for different Hopping Parameters that vary from 0 to 1. The Hopping Parameter is calculated by **Formula 4**. The On-site energy of the quantum dot is defined randomly.

As this might add unnecessary confusion, and to facilitate comparisons with the values in the Even Parity Readout Error, the results from the calculations for the Odd Parity Readout Error will be presented with the x-axis as the Hopping Parameter calculated from **Formula 3**, which will be the default Hopping Parameter from now on.

In this case, the values of the combination will go from the 0.25 Δ to 0.75 Δ. As expected, in **Graph 8** we can see what we would expect to see for the inverse of the probability of what we would expect for an Odd Parity system: maximum when the Tunneling parameters are close (near the middle of the graph), and with far smaller values from that point. This will be important to notice for future calculations and will be very useful in future calculations. It is also important to notice that, given the fact that the Parity

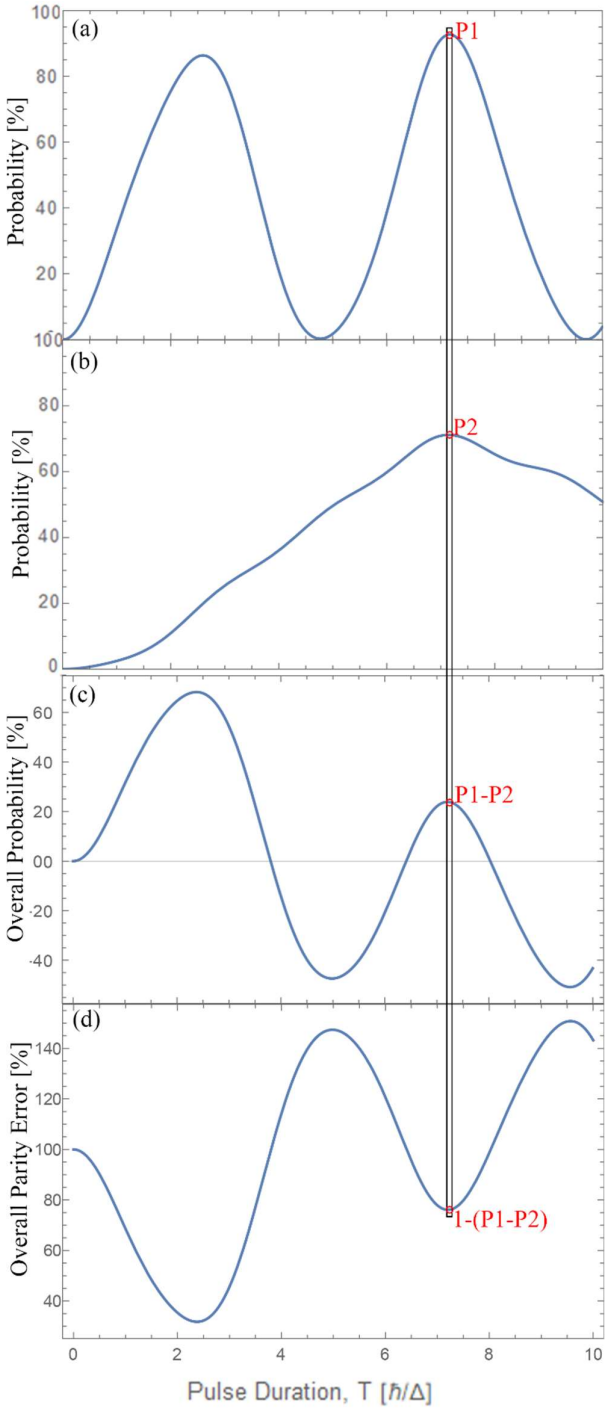

Figure 4: Calculation of the Overall Parity Readout Error from the Even and Odd Parity Probability Curve. **(a)** is the Even Probability Curve, **(b)** the Odd Probability Curve, **(c)** is the Overall Even Probability Curve and **(d)** is the Overall Even Parity Readout Error.

Readout Error of the Odd Parity system is far larger than the one for the Even, its shape will be more represented after the calculation.

While both calculations are important to understand the behavior of these curves, it is necessary to take into account how they work at the same time. As stated previously, it is important to consider the probability of both parities at any given Pulse Duration, as the probabilities of one parity affect the Parity Readout Error of the other. To observe this effect for different combinations of the Pulse Strengths, the value of the best Parity Readout Error for the Even parity where reduced by the value of the Parity Readout Error of the Odd parity at the same Pulse Duration. This gives the Overall Parity Readout Error of the Even parity system, which is an indication of how reliable is the measurement of an Even Parity in a system in a given combination of Pulse Strengths if the measurement is done at the best Pulse Duration. This can be better understood in **Figure 4**, which shows each step of the calculation of one point and presents how we go to the calculation of **Formula 7**:

- the calculation of the Probability curve for the Even and Odd parity (**(a)** and **(b)**).
- the finding of the maximum for the Even parity Probability Curve (**P1**) and the respective value on the same Pulse Duration for the Odd parity Probability Curve (**P2**).
- Subtracting the Odd Probability from the Even Probability (**P1-P2**) to create the Overall Probability (**(c)**).
- Reducing the Overall Probability from 1 to get the Overall Parity Readout Error (**1-(P1-P2)**).

$$Overall\ Parity\ Readout\ Error\ (T) = 1 - |P_{even}(T) - P_{odd}(T)|[\%]$$

Formula 7: Formula for the calculation of the Overall Parity Readout Error from the maximum of the Probability Curve for the Even Parity (P_1) and the point int the Odd Probability Curve of the Odd Parity (P_2).

The Optimal Parity Readout Error for any system is the minimum of this curve. Ideally, we would find a combination of Pulse Strengths in which the Parity Readout Error for the Even parity is 0%, but the Odd Parity Readout Error is 100%, making the Overall Parity Readout Error also 0%. It is also possible that there is a bigger value than 100%, which means that at that combination of Pulse Strengths would there be a bigger probability of finding the system at Odd parity than at Even. Due to the behavior seen in **Graph 8**, in which the Odd Parity Readout Error will have its highest point at the point where both tunneling parameters are the same, this point will always appear as one of the points with the best Overall Parity Readout Error.

Calculating to find the Overall Parity Readout Error for the lowest Pulse Duration possible we get **Graph 9**, which shows clearly the expected lower point at the middle point of the graph, where both Pulse Strengths are the same. Given that this simulation keeps one of the Pulse Strengths at 0.5 Δ and the other varies from 0 Δ to 1 Δ, the expected values for the best Overall Parity Readout Error should at Hopping

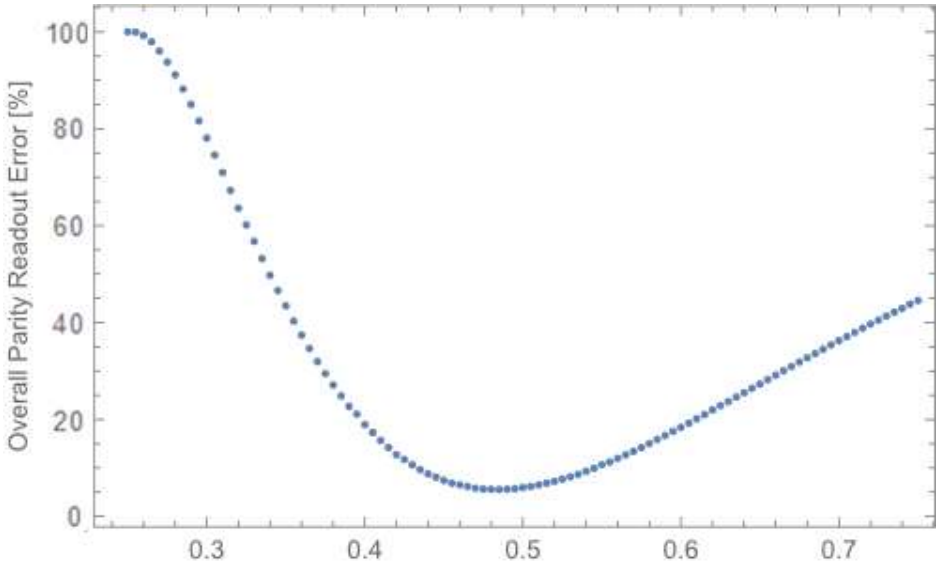

Graph 9: Overall Parity Readout Error for the lowest Pulse Duration.

Parameter of 0.5 Δ. Interestingly, the best Overall Parity Readout Error found was not at 0.5 Δ, but at 0.49 Δ, with an Overall Parity Readout Error 5.4% and a Pulse Duration of 3.34 ħ/Δ.

3.2. Finding the best Pulse Strength combination

After finding the Hopping Parameter with the best Overall Parity Readout Error, it can be explored which combination of Pulse Strengths, if any at all, produces better results of Overall Parity Readout Error.

As the Hopping Parameter is calculated from the Pulse Strengths of each connection to the quantum dot by **Formula 3** and **2** for the Even and Odd parity systems, respectively, it could be expected that, as long as the combination of the Pulse Strengths is the same, the Probability Curves would stay the same. It is, however, not true. The interaction between the Pulse Strengths in each connection goes beyond the value of the Hopping Parameter, and different Pulse Strengths, even with the same Hopping Parameter, might have different results.

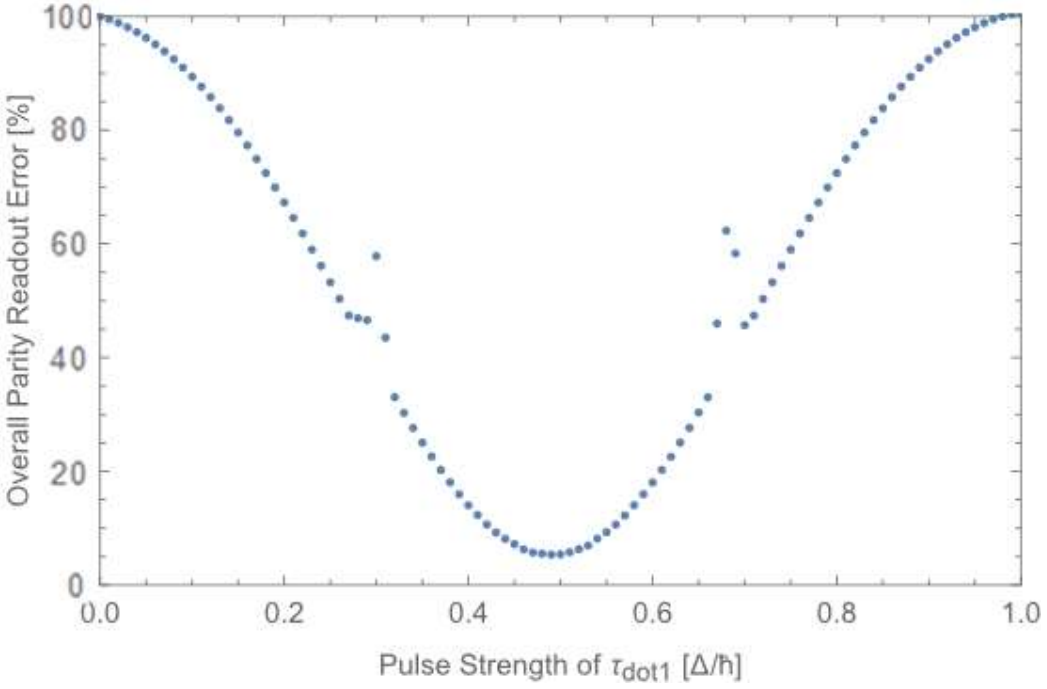

Graph 10: Overall Parity Readout Error for the low Pulse Duration with the same Hopping Parameter of 0.49

To verify it we simulated multiple different possible combinations of Pulse Strengths that would end with the same Hopping Parameter we found in the previous section to have the best Overall Parity Readout Error (0.49 Δ). The simulation was done by varying both Pulse Strengths so after they went through **Formula 4** they would have the same Hopping Parameter in all cases. This was done by progressively increasing one of the Pulse Strengths from 0 Δ, while the other progressively reduced from the double of the Hopping Parameter (0.98, in this case) so their average would remain the same. This calculation guarantees a symmetrical nature to the results, centered around the Hopping Parameter of 0.49 Δ.

Graph 10 shows the result in the calculation, and its lowest point is found at the Hopping Parameter of 0.49 Δ, with an Overall Parity Readout Error of 5.3% and a Pulse Duration of 3.35 ħ/Δ.

4. CONCLUSION

Majorana Wires, and the Majorana anyons itself, are on the cutting edge of technology and even of scientific knowledge itself. While many advances and developments have been and are being done in this field[14, 16, 17, 18], including prototypes, simulations are still one of the best ways to test and comprehend and the behavior of such systems and how to optimize them to the point they are a viable option to replace current systems.

In the simulations presented in this work, we explored different variations of the system for a Majorana Wire, taking into account different variables that affect the results of the system as well as different parts of the design of the system. As many have observed before[9, 16, 19], the two-fold degeneracy that is necessary for the Majorana Wire to have its properties that make are interesting for quantum computing, creates a

special difficulty for the readout. The solution explored on this, and other[19], works is to add a quantum dot to the system, allowing that the fermions in the systems move to outside of the positive conditions, allowing the parity to be converted into readable charge. This elegant solution allows to use of the special qualities of the Majorana Wire and opens the door for this system to become a real hardware, but also opens the necessity to explore and improve the readout results of such devices. This is, however, a still very new technology, and due to its quantum nature, mathematically complex and expensive to produce physically, simulations like the ones presented in this work are one of the best ways to better understand how to make these readouts efficient and reliable.

What we observed in this work is that any potential work with this system will need to balance 2 important factors: the Pulse Duration and the Parity Readout Error (and the Overall Parity Readout Error, if the system uses two different Pulse Strengths). The latter is certainly more important than the former, as it directly affects the reliability of the system, but the former must not be forgotten. Lower Pulse Strengths can produce considerably better Parity Readout Errors but at the cost of large Pulse Durations, which would certainly harm the efficiency of these devices. Among the challenges to balance these two that will certainly be explored is the choice of the Pulse Strength, if such will be kept the same or different combinations will be taken.

After many simulations, we found what we believe to be the best results of Pulse Duration and Parity Readout Error, but we are certain that future works can improve these values, although we do not believe that they can be much improved without further change into the system itself. Therefore, we believe that further significant development in the field will happen on investigating how to improve the design of the

Majorana Device itself, which many are already working into[15], and to combat the main factors that cause this Parity Readout Error in the first place.

ACKNOWLEDGMENTS

Firstly, I thank all who helped me to write this work, from my Supervisors who helped me so much with so many doubts, to all friends and coleagues who helped cheking for errors, confirming information, and helping in countless ways.

Secondly, I want to thank all who helped me to get where I am today. My father, who started the fire of my curiosity and courage which made me the man I am today. My brother, who helped me to develop my mind with so many debates and discussions. And my teachers, who taught me so much about the world.

Thirdly, to all who gave me the support to do what I love, from friends who help me to keep my sanity, and to my girlfriend, who gives me more support than I could ever ask.

I also want to thank ELTE for welcoming for the second time and giving me the opportunity and honour to study for my Master's degree, and the Tempus Foundation for the opportunities that me and many friends had thanks to the Stipendium Hungaricum.

REFERENCES

[1] I. Cutress. “Better Yield On 5Nm Than 7Nm’: TSMC Update On Defect Rates For N5.” Anandtech. Available at: <https://www.anandtech.com/show/16028/better-yield-on-5nm-than-7nm-tsmc-update-on-defect-rates-for-n5> (2020). [Accessed Dec 10, 2020].

[2] P. G. Emma, "Understanding some simple processor-performance limits," in IBM Journal of Research and Development **41-**3, 215-232, (1997).

[3] R. Courtland. “Transistors Could Stop Shrinking In 2021”. IEEE Spectrum. Available at: <https://spectrum.ieee.org/semiconductors/devices/transistors-could-stop-shrinking-in-2021> (2016) [Accessed December 11 2020].

[4] D. Johnson. “One-Nanometer Gate Dimensions For Transistors Have Been Achieved”. IEEE Spectrum. Available at: <https://spectrum.ieee.org/nanoclast/semiconductors/devices/onenanometer-gate-dimensions-for-transistors-have-been-achieved> (2016). [Accessed December 10, 2020].

[5] P. Benioff. “The computer as a physical system: A microscopic quantum mechanical Hamiltonian model of computers as represented by Turing machines”. Journal of Statistical Physics **22-** 5, 563-591, (1980).

[6] F. Arute, K. Arya, R. Babbush, et al. “Quantum supremacy using a programmable superconducting processor”. Nature **574**, 505–510, (2019).

[7] H.-S. Zhong, H. Wang, Y-H. Deng, et al. “Quantum computational advantage using photons”. Science **370**, 1460-1463. (2020).

[8] D. Castelvecchi. “Welcome anyons! Physicists find best evidence yet for long-sought 2D structures.” Nature **583**, 176-177, July 3, (2020).

[9] V. T. Lahtinen, J. K. Pachos. “A Short Introduction to Topological Quantum Computation”. SciPost Physics. 3, **021** (2017).

[10] N. Kumar, S. N. Guin, Manna, Kaustuv, M., et al. “Topological Quantum Materials from the Viewpoint of Chemistry”. Chemical Reviews, American Chemical Society, **Article ASAP**. (2020).

[11] N. Savage. “Topology Shapes a Search for New Material: The quest for quantum effects in matter moves from theory to practice”. ACS Cent. Sci. **4**, 523-526. (2018).

[12] E. Majorana, L. Maiani. “A symmetric theory of electrons and positrons. Physical Society (eds) Ettore Majorana Scientific Papers”. Springer, Berlin, Heidelberg., 201–233. (2006).

[13] S. Manna, P. Wei, Y. Xie, et al. “Signature of a pair of Majorana zero modes in superconducting gold surface states”. PNAS **117**-16, 8775-8782. (2020).

[14] M. Baranov. “Lecture 2: Majorana Fermions as an example of non-Abelian Anyons”. [PowerPoint Presentation]. Anyon Physics of Ultracold Atomic Gases. (2018). Available at <http://users.physik.fu-berlin.de/~pelster/Anyon3/baranov-slides2.pdf>.

[15] A. Y. Kitaev. “Unpaired Majorana fermions in quantum wires”. Physics-Uspekhi **44**, 131–136 (2001).

[16] H. Zhang, D. E. Liu, M. Wimmer, L. P. Kouwenhoven. “Next steps of quantum transport in Majorana nanowire devices”. Nature Communications **10**, 5128. (2019).

[17] J. Alicea, Y. Oreg, G. Refael, F. von Oppen, M. P. A. Fisher. “Non-Abelian statistics and topological quantum information processing in 1D wire networks”. Nature Physics **7**, 412–417, (2013).

[18] I. Fadelli. “The observation of photon assisted tunneling signatures in Majorana wires”. Phys.org, Available at <https://phys.org/news/2020-05-photon-assisted-tunneling-signatures-majorana-wires.html>. (2020). [Accessed 18 December 2020].

[19] A. Pályi, G. Széchenyi. “Parity-to-charge conversion for readout of topological Majorana qubits”. Phys. Rev. B **101** (2020).

[20] F. Chen, S. Matern, “Kitaev Chain”. University of Cologne (2014).